HHS Public Access

Author manuscript

Oncogene. Author manuscript; available in PMC 2016 October 28.

Published in final edited form as:

Oncogene. 2016 October 27; 35(43): 5608–5618. doi:10.1038/onc.2015.516.

A Novel Association of Neuropilin-1 and MUC1 in Pancreatic Ductal Adenocarcinoma: Role in Induction of VEGF Signaling and Angiogenesis

Ru Zhou[1], **Jennifer M Curry**[1], **Lopamudra Das Roy**[1], **Priyanka Grover**[1], **Jamil Haider**[2], **Laura J. Moore**[1], **Shu-ta Wu**[1], **Anishaa Kamesh**[1], **Mahboubeh Yazdanifar**[1], **William A. Ahrens**[3], **TinChung Leung**[2], and **Pinku Mukherjee**[1]

[1]Department of Biological Sciences, University of North Carolina at Charlotte, Charlotte, NC, USA

[2]Julius L. Chambers Biomedical Biotechnology Research Institute, North Carolina Central University, Kannapolis, NC, USA

[3]Section of Hepatobiliary and Pancreas Surgery, Department of Surgery, Carolinas Medical Center, Charlotte, NC, USA

Abstract

We report that MUC1, a transmembrane glycoprotein that is overexpressed in >80% of pancreatic ductal adenocarcinoma (PDA) induced a pro-angiogenic tumor microenvironment by increasing the levels of neuropilin-1 (NRP1, a co-receptor of VEGF) and its ligand, VEGF. Expression of tumor-associated MUC1 (tMUC1) positively correlated with NRP1 levels in human and mouse PDA. Further, $tMUC1^{hi}$ PDA cells secreted high levels of VEGF and expressed high levels of VEGF receptor 2 and its phosphorylated forms as compared to $tMUC1^{low/null}$ PDA. This enabled the $tMUC1^{hi}/NRP1^{hi}$ PDA cells to a) induce endothelial cell tube formation, b) generate long ectopic blood vessels and c) enhance distant metastasis in a zebrafish xenograft model. Concurrently, the proteins associated with epithelial to mesenchymal transition, N-cadherin and Vimentin, were highly induced in these $tMUC1/NRP1^{hi}$ PDA cells. Hence, blocking signaling via the NRP1-VEGF axis significantly reduced tube formation, new vessel generation, and metastasis induced by $tMUC1^{hi}$ PDA cells. Finally, we show that blocking the interaction between $VEGF_{165}$ and NRP1 with a NRP1 antagonist significantly reduced VEGFR signaling and PDA tumor growth *in vivo*. Taken together, our data suggests a novel molecular mechanism by which tMUC1 may modulate NRP1-dependent VEGFR signaling in PDA cells.

Correspondence: Dr. Pinku Mukherjee, Department of Biological Sciences, University of North Carolina at Charlotte, 9201 University City Boulevard, Charlotte, NC 28223, USA. Phone: 704-687-5465; Fax: 704-687-3122; pmukherj@uncc.edu.

Conflicts of Interest

Dr. Pinku Mukherjee is a board member in OncoTab. Dr. Lopamudra Das Roy is an employee of OncoTab. The other authors declare no conflict of interest.

Supplementary Information accompanies the paper on the Oncogene website (http://www.nature.com/onc).

Keywords

tMUC1; NRP1; VEGF; pancreatic ductal adenocarcinoma; angiogenesis

Introduction

Angiogenesis is a complex process of new blood vessel formation from pre-existing vascular networks by capillary sprouting. Full execution of angiogenesis requires complex signaling via vascular endothelial growth factor (VEGF) and its receptors.[1] VEGF-A is one of the major stimulators of angiogenesis induced by hypoxia during oncogenic process. Within the VEGF-A family of growth factors, $VEGF_{165}$ is well characterized and mediates angiogenic sprouting and endothelial cell organization *in vitro* and *in vivo*.[2, 3]

Three structurally homologous tyrosine kinase VEGF receptors are VEGFR1 (Flt-1), VEGFR2 (KDR/Flk-1), and VEGFR3 (Flt-4). The majority of the endothelial cell responses to VEGF including differentiation, proliferation, migration, and formation of the vascular tubes are mediated through VEGFR2.[4–7] VEGFR1 is speculated as a decoy receptor, sequestering VEGF signaling through VEGFR2.[4, 5] VEGFR3 expression is restricted mainly to the lymphatic endothelium of adult tissues. It binds VEGF-C and VEGF-D, but not VEGF-A, and is thought to control lymphangiogenesis.[8, 9]

Neuropilins (NRPs) are transmembrane receptors without a tyrosine kinase domain and can act as co-receptors for VEGF family of pro-angiogenic cytokines[10] and the class 3 semaphorin (Sema3) family of axon guidance molecules.[11] NRPs are gaining much attention as multifunctional proteins involved in normal development, immunity, and tumor progression as reviewed by Prud'homme et al.[12] NRP1 is expressed by endothelial cells, dendritic cells, regulatory T cells, several other normal cell types, as well as tumor cells.[13–15] It is a co-receptor for VEGFR2, with $VEGF_{165}$ binding to both NPR1 and VEGFR2 simultaneously.[10] It has been proposed that NRP1 may enhance $VEGF_{165}$ binding and bioactivity by forming a bridge between NRP1 and VEGFR2, bringing these receptors into close proximity, and promoting angiogenesis.[16] Neutralizing NRP1 is additive to VEGF neutralization in suppressing vascular remodeling and tumor growth.[17] Importantly, NRP1 is predominantly expressed in carcinomas (particularly those of epithelial cell origin), including carcinomas of lung, breast, prostate, pancreas, and colon.[18, 19] Over-expression of NRPs correlates with disease progression, metastatic potential and poor prognosis.[10, 19, 20]

Therefore, NRP1 is an attractive therapeutic target. A number of strategies have been evaluated by using NRP1 ectodomains or soluble NRP1 as VEGF Trap, anti-NRP1 antibodies, knockdown by siRNA, or by using a small peptide-mimetic of VEGF to selectively block VEGF binding to NRP1.[15] A heptapeptide ATWLPPR (A7R) is identified by screening a phage-displayed peptide library against an anti-VEGF-antibody that blocks $VEGF_{165}$-dependent endothelial cell proliferation.[21] A7R inhibits $VEGF_{165}$ binding to NRP1 but not to VEGFR1, VEGFR2, or heparin. *In vivo* treatment with A7R reduces blood vessel density and endothelial cell area, and suppresses the growth of MDA-MB-231 xenografts in nude mice.[22]

Pancreatic ductal adenocarcinoma (PDA) is the fourth leading cause of cancer-related death in the United States.[23] The transmembrane glycoprotein Mucin1 (MUC1) is overexpressed and aberrantly glycosylated in more than 80% of metastatic PDA and is associated with poor prognosis.[24] We and others have shown that this tumor-associated form of MUC1 (tMUC1) enhances invasiveness of pancreatic cancer cells by inducing epithelial to mesenchymal transition (EMT) and that these tumors express high levels of VEGF, cyclooxygenase-2, prostaglandin E2, and platelet-derived growth factor (PDGF).[25, 26] Lack of tMUC1 in PDA mice prevents tumor progression and metastasis and has lower levels of VEGF.[25, 27] In addition, MUC1 overexpression has been demonstrated to promote VEGF production through insulin-like growth factor-1 (IGF-1) receptor/Akt cascades, leading to the enhanced tumor growth and angiogenesis in human breast carcinoma.[28] Thus, in this study we assess if tMUC1 induces a pro-angiogenic microenvironment in PDA and begin to elucidate the mechanism. We show for the first time that PDA cells and tumors that express high levels of tMUC1 have increased levels of NRP1 as compared to PDA with no or low levels of tMUC1. NRP1 potentiates VEGF receptor signaling and pro-angiogenic activities, thus indicative of enhanced intra-tumoral angiogenesis and disease progression. Finally, we show that blocking the interaction between $VEGF_{165}$ and NRP1 within the tumor microenvironment leads to disruption of VEGF signaling and therapeutic benefit in mouse models.

Results

Level of NRP1 expression correlates with expression of tMUC1 in human PDA

We and others have shown that tMUC1 is overexpressed in PDA and is associated with enhanced metastasis and poor diagnosis.[24, 25, 27, 29] Parikh et al first reported NRP1 expression in the PDA.[30] Here we first showed that tMUC1 and NRP1 were expressed in primary human PDA, but minimally in the normal pancreas (Figure 1A). The staining in the tumor was mainly restricted to the ductal epithelia. To determine if a correlation existed between tMUC1 and NRP1, we examined a panel of human PDA cell lines that endogenously express high, medium, or low tMUC1 by Western blot using an antibody against the extracellular tandem repeat of MUC1 (MUC1 TR, TAB 004). Cells expressing high endogenous tMUC1 such as CFPAC, HPAFII, and HPAC also displayed high NRP1, while cells with low endogenous tMUC1 displayed low NRP1 with the exception of Panc1 cells (Figure 1B; quantitation data shown as Supplementary Figure 1A). Since NRP1 is a co-receptor of VEGF and signaling through VEGFR2 is critical for the angiogenic signaling to occur,[10] we examined the levels of VEGFR2 in the same cell lines. However, the correlation between tMUC1 and VEGFR2 levels were not consistent among the cell lines (Figure 1B).

Thus, we determined if MUC1 regulated the expression of NRP1 by conducting gain and loss of function studies. The full-length human MUC1 was stably transfected into two $tMUC1^{low}$ cells, a human pancreatic cell line BxPC3 and a mouse pancreatic cell line Panc02. The overexpression of tMUC1 was confirmed by flow cytometry (Figure 1C, left panel) and by Western blotting (Figure 1C, right panels). In BxPC3.MUC1 and Panc02.MUC1 cells, tMUC1 overexpression induced significantly higher expression of NRP1 than their control counterparts carrying the empty vector (BxPC3.Neo and Panc02

Neo) (Figure 1C, right panels; Supplementary Figure 1B). On the other hand, three tMUC1^{hi} cell lines (HPAC, CFPAC and HPAFII) treated with MUC1-specific siRNA showed dramatically reduced MUC1, and moderately decreased NRP1 expression although not statistically significant (Figure 1D and 1E). Protein expression of NRP1 and tMUC1 relative to β-actin was shown in Figure 1E. Whether this regulation was direct or indirect was yet to be delineated.

Increased expression of NPR1, VEGFR, and VEGF in tumor cells derived from spontaneous Muc1^{+} PDA mouse

We have established two mouse PDA cell lines, KC and KCKO, from spontaneously arising PDA tumors in WT (Muc1 intact) and in Muc1 null mice respectively.[27] A gene microarray was conducted in these two cells as well as in BxPC3.MUC1 and BxPC3.Neo cells. Among those altered genes, KC and BxPC3.MUC1 cells showed higher NRP1 levels than those in KCKO and BxPC3.Neo cells (data not shown). Thus, we confirmed expression of Muc1 and NRP1 in KC cells by flow cytometry (Figure 2A) and Western blot (Figure 2B; Supplementary Figure 2). Compared to KCKO, KC cells displayed higher levels of Muc1 (Figure 2A, left panel, and 2B) and moderately higher level of NRP1 (Figure 2A, right panel, and 2B). In addition, Muc1^{hi} KC cells expressed higher levels of VEGFR2 than the Muc1-null KCKO cells (Figure 2B).

Further, KC cells secreted significantly higher levels of VEGF than KCKO cells (Figure 2C), which could be partially inhibited by NRP1 antagonist A7R (Figure 2D) without affecting cell numbers (Figure 2E). These data may suggest that the NRP1-VEGFR2 signaling may positively regulate VEGF secretion and this may be partially dependent on Muc1 expression in PDA cells.

Muc1-expressing PDA cells promote endothelial cell tube formation through VEGF signaling

Since endothelial tube formation assay is used as a surrogate for angiogenesis, we studied the influence of conditioned medium from tumor cells on endothelial cell tube formation and whether signaling via NRP1 was required. As shown in Figure 3A, murine endothelial 2H11 cells endogenously expressed high levels of NPR1 and VEGFR2. Functionally, capillary-like structure formation is one of the most important morphological changes during angiogenesis, and can be quantitated by counting the sprouting and branching of endothelial cells.[31] As compared to conditioned media from KCKO cells, the media from KC cells induced enhanced tube formation in 2H11 cells (5hr post incubation) (Figure 3B). Tube formation was partially suppressed by blocking NRP1 activity with A7R or by neutralizing VEGF (Figure 3D). Combination of A7R with anti-VEGF antibody had additive effect in significantly inhibiting the tubular structure formation on the matrigel basement (Figure 3D). The quantitative results were shown in Figure 3C and Figure 3E. In addition, direct pre-treatment of KC cells with A7R effectively decreased VEGF secretion in the supernatant (Supplementary Figure 3A). Further, the supernatant from A7R pretreated KC cells induced significantly less tube formation (Supplementary Figure 3B and 3C).

NRP1 plays a critical role in promoting ectopic blood vessel formation and enhancing metastatic spread in a zebrafish embryo xenograft model

Since MUC1/VEGF signaling increased the *in vitro* endothelial cell tube formation (Figure 3), we evaluated the role *in vivo*. The zebrafish/tumor xenotransplantation has been characterized as a whole-animal model to study tumor angiogenesis *in vivo*.[32] In this zebrafish model, we studied whether the xenograft of tMUC1^{hi}/NRP1^{hi} cells affected formation of ectopic blood vessel (number and length) one day post tumor cell injection. We showed for the first time that human PDA cell line, BxPC3.MUC1 promoted a significant increase in the number and length of ectopic vessels than its BxPC3.Neo counterpart (Figure 4A and 4B, see arrows). Furthermore, compared to BxPC3.Neo cells, BxPC3.MUC1 cells exhibited significantly more metastasis by showing their migration away from the site of injection (Figure 4C and 4D). To elucidate the role of NRP1 in the tumor-induced angiogenesis and metastasis, BxPC3.MUC1 cells with or without A7R treatment were injected into the zebrafish embryo. A known angiogenesis inhibitor, PTK787 was used as a positive control which blocks all known VEGF receptor tyrosine kinases.[33, 34] We observed moderately reduced growth of ectopic vessels and tumor cell metastasis in the embryos treated with PTK787. However, A7R treatment significantly blocked ectopic vessel formation and metastatic spread, implicating a critical involvement of NRP1 (Figure 4E).

Muc1 up-regulates NRP1 and creates a pro-angiogenic niche *in vivo*

To further demonstrate that high expression of Muc1 may create a pro-angiogenic niche *in vivo*, spontaneously arising tumors from PDA mice were assessed for the expression of angiogenesis-related proteins by IHC. Expression of NRP1, VEGF, CD31, and PCNA was higher in the spontaneously arising KC than KCKO tumors (Figure 5A). It was noted that the NRP1 and PCNA expressions were mainly localized to the epithelial layer of ductal region.

To understand the mechanism of NRP1-associated VEGF signaling, lysates from KC and KCKO tumors were analyzed for the VEGFR2 phosphorylation and proteins of other angiogenesis-related pathways. Western blot data were summarized in Figure 5B and quantitated (Supplementary Figure 4). Interestingly, not only were the levels of NRP1 and VEGFR2 significantly lower in the KCKO tumors, the phosphorylation of VEGFR2 at tyrosine sites of 1175 and 996 were also lower (Figure 5B) which was likely due to the lower level of receptor itself. Tyrosine1175 is essential for VEGF-induced kinase activation, including PLC-γ and MAPK, and for VEGF-induced proliferation of endothelial cells.[35] Other sites of tyrosine autophosphorylation include Tyr996 along with Tyr996, 1054, and 1059 (ref[36, 37]). Moreover, levels of N-Cadherin and Vimentin were higher while E-Cadherin was lower in KC versus KCKO tumors (Figure 5B), suggestive of EMT transition. Together, the data suggested that lack of Muc1 impaired the expression of NRP1 and VEGFR2, and thereby down-regulated the angiogenic and EMT signaling which are potential pre-requisites for metastasis.

Blockade of NRP1 signaling attenuates tMUC1^{hi} tumor growth *in vivo*

Based on the above findings, we lastly validated the activity of NRP1 antagonist A7R in tumor-bearing mice. In the immune-competent C57BL/6 mice, the growth of KC tumor was

significantly reduced over time by subcutaneous injection of A7R (Figure 6A). Nude mice bearing BxPC3.MUC1 tumors also responded to the mono-therapy with A7R, displaying significantly lower tumor burden and with 4 out of 7 mice showing a complete response (Figure 6B). Western blot data from A7R-treated KC tumors further confirmed that the *in vivo* inhibition of NRP1 activity by A7R led to the reduction of VEGFR2 activation, as evidenced by decreased phosphorylation at Tyr1175 (Figure 6C; Supplementary Figure 5). And interestingly, the protein level of NRP1 was clearly reduced by suppressing its own activity, suggesting a possible autocrine regulation of NRP1 expression via the VEGFR2 signaling.

Primary human PDA tumors express varying levels of NRP1

The tumors from pancreatic cancer patients expressed tMUC1 and NPR1 as shown in Figure 1A. In addition, the IHC staining verified the presence of pro-angiogenic factors including VEGF, CD31, and PCNA in the tumors (Figure 7A). Using a pancreas cancer tissue array, tMUC1 expression was detected in all PDA tissues restricted to the ductal epithelia, but the intensity of expression varied (Supplementary Figure 6A). Normal adjacent pancreas tissue also showed MUC1 staining but was restricted to the acinar secretions and absent in the ductal epithelial cells (data not shown). Similarly, NRP1 was expressed at varying levels in the tumors from the same 40 PDA patients. Closely but not exactly, we found the higher the tMUC1 expression in PDA, the stronger the NRP1 expression (Figure 7B and C; Supplementary Figure 6). A nonparametric Spearman correlation of 0.70 was achieved with n=65 tissue-cores which was highly significant ($P < 0.0001$) and indicated a positive association between the MUC1 and NRP1 in human PDA.

Discussion

To the best of our knowledge, we are the first to demonstrate that tMUC1 in PDA may play a role in VEGF signaling through the up-regulation of VEGF co-receptor NRP1 (Figure 1 and 2), and that blocking the interaction between $VEGF_{165}$ and NRP1 within the tumor microenvironment has therapeutic benefit *in vivo* (Figure 6). Positive staining for NRP1 in n=41 patient PDA sections (Figure 7) substantiates the clinical relevance of this protein as a potential therapeutic target.

Our previous study has shown that the spontaneously arising Muc1/MUC1-expressing PDA mice developed aggressive tumors and had poor survival than PDA mice null for Muc1/MUC1.[27] tMUC1 enhances the molecular process of EMT, promotes the expression of pro-angiogenic and pro-metastatic proteins in PDA,[25] and make tumors more drug resistant.[26, 38] In this study, we found a positive correlation between tMUC1 expression and NRP1 level in PDA cell lines and tumors (Figure 1 and 2), which may suggest the contribution of NRP1 to the malignant progression of $tMUC1^{hi}$ tumor.

It has been proposed that VEGF can signal through NRP1 in tumor and endothelial cells by 1) autocrine signaling in tumor cells to inhibit tumor cell apoptosis, 2) paracrine signaling from tumor cells to endothelial cells for angiogenesis induction, or 3) juxtacrine signaling in both cells in which VEGF may bind to NRP1 on tumor cells and bind to VEGFR2 on endothelial cells simultaneously for NRP1 induction of angiogenesis and tumor growth.[16, 39]

We found that although blockade of NRP1 activity inhibited VEGF-induced Erk and Akt activation in KC cells (data not shown), the cell proliferation and survival were not affected (data not shown) indicating that the NRP1-dependent Erk and Akt activation may play roles in other aspects of tumor growth. We further found that NRP1 was involved in VEGF production probably by VEGF self-regulation through VEGFR-NRP1 signaling. The partial reduction of VEGF by NRP1 antagonism in $tMUC1^{hi}$ cells might emphasize its role as a co-receptor for VEGFR2, but also suggested the involvement of other signaling cascades. Woo et al has reported the MUC1 overexpression/IGF-1-IGF-1R/Akt/VEGF signaling in the human breast carcinoma models[28], which could be one of the possibilities involved in our models. Although we did not prove the juxtacrine signaling between tumor cells and endothelial cells here, it was obvious from Figure 3C that PDA cells could directly promote the formation of capillary structure in endothelial cells through soluble factors. VEGF was not the only soluble contributor for tube formation since neutralization of VEGF only partially suppressed the tube induction. However, combination of A7R treatment with VEGF neutralization displayed additive benefit in suppressing endothelial tube formation (Figure 3E). Since blocking NRP1 on either tumor cell (Supplementary Figure 3) or endothelial cell (Figure 3D and 3E) effectively decreased the tube formation, it shed light on the NRP1 as a promising target for tumor-associated angiogenesis.

Furthermore, BxPC3 cells with high tMUC1/NRP1 could enhance new vessel formation in the zebrafish embryo xenotransplantation model (Figure 4A and B), and they were also highly migratory (Figure 4C and D). These activities were largely dependent on NRP1 as demonstrated by its blockade (Figure 4E). Together, our data strongly suggested that tMUC1 increased NRP1 level, which was essential for tumor-associated angiogenesis and metastasis. Despite the advantages and simplicity of the zebrafish model, the spontaneously arising PDA mouse model resembles more closely the human disease. We found minimal expression of pro-angiogenenic proteins (VEGF, NRP1, CD31, and PCNA) in tumors from $Muc1^{null}$ KCKO mice when compared with tumors from $Muc1^{hi}$ KC mice (Figure 5A). In addition, the NRP1, VEGFR2 and its activation forms of Tyr1175 and Tyr996 were significantly higher in the KC versus KCKO tumors (Figure 5B). These data strongly indicate that increased NRP1/VEGF signaling in $tMUC1^{hi}$ tumors correlates with enhanced angiogenesis *in vivo*. However, since both tumor cells and endothelial cells express NRP1 and other VEGF signaling molecules (Figure 2 and 3), the contribution of intra-tumoral endothelial cells for their expression and activation could not be excluded. In addition, there was also biased expression of EMT markers in KC tumors versus KCKO tumors, which may favor the KC cell invasion and metastasis. In our early publication, we found that the CT of MUC1 translocates to the nucleus in association with β-catenin, represses E-Cadherin expression, and upregulates the level of the EMT inducers Snail, Slug, Vimentin, and Twist.[25] VEGF and NRP1 have been found to directly promote EMT.[40] Besides, it has been proposed that NRP1 enhances signaling in three major pathways that are linked to EMT, i.e., transforming growth factor β1 (TGFβ1), Hedgehog and hepatocyte growth factor (HGF) and its receptor (cMet).[12] Together, we speculate that in the presence of high tMUC1, the increased NRP1 may play dual roles in both VEGFR2-associated angiogenesis and EMT-led metastasis, resulting in the aggressive tumor growth.

Finally, targeting NRP1 activity with a 7-mer peptide, A7R, inhibited the tMUC1^{hi} tumor growth of both mouse and human origin but had little effect on tMUC1-low cells (data not shown). A7R competes with $VEGF_{165}$ for binding to NRP1 without affecting its binding to VEGFR2.[22] As a result, it partially prevented VEGFR2 activation *in vivo* (Figure 6C), decreased NRP1 protein level and in turn led to retardation of tumor growth (Figure 6A and 6B). Furthermore, we observed high expression of these pro-angiogenic factors including NRP1, VEGF, and CD31 in spontaneous mouse PDA tumors as well as in the primary human PDA tissues signifying the clinical relevance of this study. It may thus be promising to target NRP1 along with other standard therapies for treatment of tMUC1^{hi} PDA. As recently discovered, NRP1 and NRP2 actually have much broader activities. They bind TGFβ1 and its receptors, HGF/cMet, PDGF and its receptors, fibroblast growth factors, and integrins. They also promote Hedgehog signaling. These ligands and pathways are all relevant to angiogenesis and wound healing. In the immune system, the NRPs are expressed primarily on dendritic cells and regulatory T cells, and exert mainly inhibitory effects. They promote EMT, and the survival and self-renewal of cancer stem cells.[41–43] These important functions of NRP1 are extremely relevant to this study since tMUC1 is expressed on pancreatic cancer stem cells[44] and is associated with PDGF signaling, EMT and drug resistance[25, 26, 38] in pancreatic cancer. Further, tumors with high tMUC1 shows higher prevalence of T regulatory cells and myeloid derived suppressor cell population in the tumor draining lymph nodes and tumor infiltrating lymphocytes.[45] Thus, the precise mechanism for tumor inhibition by A7R will need to be further demonstrated.

In conclusion, despite the complex role of NRP1 in endothelial and tumor cells, and in tumor progression, NRP1 may be an excellent target for treating tMUC1^{hi} PDA. Our current study lays the ground for combinational therapy of NRP1 antagonist with standard of care drugs. We recognize that previous trials with drugs targeting angiogenesis have produced serious side effects, including hypertension, thrombotic events, and allergic reactions. Several phase I studies of the human monoclonal anti-NRP1 antibody MNRP1685A in patients with solid tumors have shown its inhibition of VEGF pathway, either alone or in combination with VEGF blockade.[46–48] It is well accepted that drug delivery into the pancreas is difficult, as PDA is highly desmoplastic with dense stroma. Thus, compared to the anti-NRP1 antibody therapy, a small peptide antagonist against NRP1 is probably more effective to get into tumor. In the next study we propose targeted drug delivery by conjugating NRP1 inhibitors to a tMUC1-specific antibody and combine this with other standard chemotherapy, which might be highly efficacious for treatment of tMUC1^{hi} PDA.

Materials and Methods

Spontaneous mouse models and tissue culture

KC mice were generated in our laboratory on C57BL/6 background by mating the P48-Cre with the LSL-KRAS (G12D) mice.[49] They were further mated with the Muc1 knockout mice to generate KCKO mice.[50] The respective KC and KCKO cell lines were generated and maintained as described previously.[27] The animal study protocol was approved by the Institutional Animal Care and Use Committee of the University of North Carolina atCharlotte. Animal care and use were in compliance with institutional guidelines.

Cell culture

Selected human pancreatic cancer cell lines (CFPAC, HPAFII, HPAC, Capan1, Capan2, Panc1, HS766T, and Miapaca2) were obtained from American Type Culture Collection and cultured as instructed. BxPC3.Neo and BxPC3.MUC1 were generated as described previously,[25] Panc02.Neo and Panc02.MUC1 cells were originally gifted by Dr. Hollingsworth (University of Nebraska), and maintained in medium with Geneticin (G418; Invitrogen; Carlsbad, CA, USA). Murine endothelial 2H11 cell line was kindly provided by Dr. Didier Dreau (Department of Biological Sciences, University of North Carolina-Charlotte).

NRP1 antagonist A7R

The A7R peptide (ATWLPPR) was synthesized by Selleck Chemicals (Houston TX, USA) and also by Shengnuo Peptide USA (Menlo Park, CA, USA). A7R was dissolved in PBS and sterilized by filtration.

Small interfering RNA transfection

HPAC, CFPAC, and HPAFII cells were plated at 300 000 cells/well in six-well plates and grown to 50% confluence. Cells were transfected with human MUC1-specific siRNA (Dharmacon; Lafayette, CO, USA) or control siRNA (Cell Signaling Technologies; Danvers, MA, USA) in lipofectamine-2000 transfection reagent (Invitrogen), in accordance with the manufacturer's instructions. MUC1 and NRP1 protein levels were determined after transfection.

Flow cytometry

Cells were stained for human MUC1 with TAB004 (OncoTab Inc., Charlotte, NC[44]) conjugated with Cy5.5 (Abcam; Cambridge, MA, USA), and for mouse NRP1 with CD304-APC (Biolegend; San Diego, CA, USA). For mouse Muc1, cells were fixed in 4% paraformaldehyde (Sigma-Aldrich; St. Louis, MO, USA) and permeabilized with Triton-X 100 (Fisher Scientific; Waltham, MA, USA), stained with CT2 antibody (kind gift from Dr. Gendler at Mayo Clinic Arizona[51]), followed by PE-conjugated anti-Armenian hamster antibody (BD Biosciences; San Jose, CA, USA). Data was acquired on BD LSRFortessa flow cytometer (BD Biosciences), and analyzed with FlowJo software (version 8.8.7).

ELISA

KC and KCKO cells were plated overnight, followed by serum-starvation for 24hr. Cell conditioned medium (culture supernatant) was collected and frozen at -80°C. For A7R treatment, various concentrations of A7R were added into serum-free medium for 24hr. The VEGF concentration was determined by ELISA (R&D Systems; Minneapolis, MN, USA).

MTT assay

KC cells were plated as triplicate overnight, and treated with various concentrations of A7R in serum-free medium for 24hr. The cell viability was determined by Vybrant® MTT Cell Proliferation Assay Kit (Life Technologies, Grand Island, NY, USA).

Tube formation assay

A 96-well tissue culture plate was coated with 50μl/well of growth factor-reduced matrigel (BD Biosciences), which was allowed to solidify at 37°C for 30 min. 2H11 mouse endothelial cells (4×10^4 cells/50μl/well) was added to the matrigel in the presence of different treatments and incubated at 37°C for varying times. Cells were photographed using a phase contrast microscope (Nikon USA, Garden City, NY, USA). Tube formation was quantified by counting the average number of branching points in four randomly selected fields, using 40× magnification.

Western blot

Western blot was performed as previously described.[25] CT2 and TAB004 antibodies were used. NRP1 antibody was purchased from Abcam and β-actin antibody from Santa Cruz Biotechnology (Dallas, Texas, USA). Other antibodies were purchased from Cell Signaling Technologies. The density of signal was quantitated by ImageJ (version 1.49o) and summarized as supplementary data.

Immunohistochemistry staining (IHC)

Tissues were fixed in 10% neutral-buffered formalin. Paraffin-embedded blocks were prepared by the Histology Core at the Carolina Medical Center, and 4-micron thick sections were cut for staining. IHC was performed as described previously.[25] Representative images were taken at 100× or 200× magnification and quantitated by CaresBio Laboratory (Shelton, CT, USA). Antibodies for NRP1 and CD31 were from Abcam, and antibodies for VEGF and PCNA were from Santa Cruz. HRP-conjugated TAB 004 was used for tMUC1 staining at 1:750 dilution. The normal and malignant patient pancreas tissues were kindly provided by National Cancer Institute. The tissue microarray (TMA) slides were purchased from US Biomax (Rockville, MD, USA). The staining procedure for NRP1 was adapted from literature published previously.[52] The TMA slides were deparaffinized in xylene, rehydrated in a series of ethanol (100%, 95%, and 70%) followed by tap water, PBS, and then subjected to antigen retrieval in 99°C water bath for 40min. The activity of endogenous peroxidases was blocked by 2% hydrogen peroxide for 15min. The slides were washed twice in PBS, followed by PBS containing 0.05% Triton X-100, for 5min each wash. The slides were blocked with 5% normal goat serum for 1hr at room temperature, and then incubated with diluted NRP1 antibody (1:200) overnight at 4°C. The tissues were washed twice in PBS and incubated with secondary goat anti-rabbit antibody (1:100). The signal was enhanced by one-step incubation with Vectastain Elite ABC reagent (Vector Laboratories, Burlingame, CA, USA) for 30 min at room temperature. The substrate DAB was added for 5min, followed by counterstaining with Mayer's hematoxylin solution. The TMA tissues were then dehydrated in a series of ethanol, immersed into xylene, and mounted using Permount (Fisher Scientific).

Zebrafish/Tumor xenograft model

The transplantation of tumor cells into zebrafish embryos is described in details by Moshal et al.[53] In brief, tumor cells were stained with chloromethylbenzamido-DiI (CM-DiI showing red fluorescence, Invitrogen), and injected at the superficial location of the yolk

near to the perivitelline space of the 2-day old zebrafish embryos. Six days later, the metastatic spread of the CM-Dil-labeled tumor cells from the site of injection represented metastasis. Imaging was performed using an Olympus MVX10 MacroView Fluorescence Microscope (Olympus, Center Valley, PA) with Hamamatsu C9300-221 high-speed digital CCD camera (Hamamatsu City, Japan).

The tumor-induced angiogenic response was evaluated on the new vasculature sprouting from the developing subintestinal vessels by using whole-mount alkaline phosphatase staining. One day after transplantation, the zebrafish embryos were fixed in 4% paraformaldehyde and stained for endogenous alkaline phosphatase activity using nitroblue tetrazolium and 5-bromo-4-chloro-3-indolyl phosphate (Roche Applied Science, Indianapolis, IN). Images were taken by using Nikon SMZ1500 fluorescent stereomicroscope with digital color camera DXM1200c (Nikon Instruments, Lewisville, TX, USA). The number and length of the newly formed ectopic blood vessels were quantitated by using NIS-Element AR software (Nikon Instruments) for analysis. N=100 embryos/each group.

Where appropriate, A7R at 1mM was mixed with tumor cell suspension right before cell injection. PTK787 (Santa Cruz Biotechnology) at 0.1μM was added into the embryo culture medium right after tumor cell injection. N=33 embryos/each group.

In vivo tumor growth

Eight to ten weeks old C57BL/6 mice were subcutaneously (s.c.) injected with KC cells at 4×10^6cells/mouse (in 100μl PBS) into the flank. Nude mice (J:NU) were s.c. injected with BxPC3.MUC1 cells at 4×10^6cells/mouse (in 100μl PBS) into the flank. When tumor reached approximately 30–60mm^3, the mice were treated s.c. with A7R at 100mg/kg (for KC tumor) or 20mg/kg (for BxPC3.MUC1 tumor) in 100μl PBS, close to tumor, three times a week. Caliper measurements were taken by investigator and tumor weight was calculated according to the formula: weight (mg) = [length in mm × (width in mm)^2]/2].[27] Upon sacrifice, the tumors were weighed, prepared for tissue lysates and fixed for IHC. Mice were from Jackson Laboratory, Maine, USA, and randomly assigned as 7 mice/group.

Statistical analysis

Data were analyzed with GraphPad Prism 6 software. Results were expressed as mean±SD where indicated, and were representative of two or more independent experiments. Significance was determined by unpaired student *t*-test or two-way ANOVA (*, $p< 0.05$, **, $p< 0.01$, ***, $p< 0.001$). A nonparametric Spearman correlation (SAS program) was used to determine the association between MUC1 and NRP1 in patient samples.

Supplementary Material

Refer to Web version on PubMed Central for supplementary material.

Acknowledgments

This study was supported by NIH CA118944-01A1, NIH CA173668-01, and DOD CA110832.

We thank Dr. Tim D. Eubank (Department of Internal Medicine, The Ohio State University, Columbus, Ohio, USA) for the valuable support with angiogenesis study. We thank Dr. Lloye Dillon (OncoTAB, Inc., Charlotte, NC, USA) for the critical review of the manuscript. We thank all the technicians in the animal facility for their assistance in maintaining our colonies.

Abbreviations

PDA	pancreatic ductal adenocarcinoma
tMUC1	tumor associated MUC1
NRP1	neuropilin-1
EMT	epithelial to mesenchymal transition
IHC	immunohistochemistry
PCNA	proliferating cell nuclear antigen
siRNA	small interfering RNA
Erk	extracellular signal-regulated kinase.

REFERENCES

1. Roskoski R Jr. Vascular endothelial growth factor (VEGF) signaling in tumor progression. Crit Rev Oncol Hematol. 2007; 62:179–213. [PubMed: 17324579]
2. Ferrara N, Davis-Smyth T. The biology of vascular endothelial growth factor. Endocr Rev. 1997; 18:4–25. [PubMed: 9034784]
3. Whittle C, Gillespie K, Harrison R, Mathieson PW, Harper SJ. Heterogeneous vascular endothelial growth factor (VEGF) isoform mRNA and receptor mRNA expression in human glomeruli, and the identification of VEGF148 mRNA, a novel truncated splice variant. Clin Sci (Lond). 1999; 97:303–312. [PubMed: 10464055]
4. Robinson CJ, Stringer SE. The splice variants of vascular endothelial growth factor (VEGF) and their receptors. J Cell Sci. 2001; 114:853–865. [PubMed: 11181169]
5. Park JE, Chen HH, Winer J, Houck KA, Ferrara N. Placenta growth factor. Potentiation of vascular endothelial growth factor bioactivity, in vitro and in vivo, and high affinity binding to Flt-1 but not to Flk-1/KDR. The Journal of biological chemistry. 1994; 269:25646–25654. [PubMed: 7929268]
6. Waltenberger J, Claesson-Welsh L, Siegbahn A, Shibuya M, Heldin CH. Different signal transduction properties of KDR and Flt1, two receptors for vascular endothelial growth factor. The Journal of biological chemistry. 1994; 269:26988–26995. [PubMed: 7929439]
7. Seetharam L, Gotoh N, Maru Y, Neufeld G, Yamaguchi S, Shibuya M. A unique signal transduction from FLT tyrosine kinase, a receptor for vascular endothelial growth factor VEGF. Oncogene. 1995; 10:135–147. [PubMed: 7824266]
8. Pajusola K, Aprelikova O, Korhonen J, Kaipainen A, Pertovaara L, Alitalo R, et al. FLT4 receptor tyrosine kinase contains seven immunoglobulin-like loops and is expressed in multiple human tissues and cell lines. Cancer Res. 1992; 52:5738–5743. [PubMed: 1327515]
9. Kaipainen A, Korhonen J, Mustonen T, van Hinsbergh VW, Fang GH, Dumont D, et al. Expression of the fms-like tyrosine kinase 4 gene becomes restricted to lymphatic endothelium during development. Proceedings of the National Academy of Sciences of the United States of America. 1995; 92:3566–3570. [PubMed: 7724599]
10. Wild JR, Staton CA, Chapple K, Corfe BM. Neuropilins: expression and roles in the epithelium. Int J Exp Pathol. 2012; 93:81–103. [PubMed: 22414290]
11. He Z, Tessier-Lavigne M. Neuropilin is a receptor for the axonal chemorepellent Semaphorin III. Cell. 1997; 90:739–751. [PubMed: 9288753]

12. Prud'homme GJ, Glinka Y. Neuropilins are multifunctional coreceptors involved in tumor initiation, growth, metastasis and immunity. Oncotarget. 2012; 3:921–939. [PubMed: 22948112]
13. Tordjman R, Lepelletier Y, Lemarchandel V, Cambot M, Gaulard P, Hermine O, et al. A neuronal receptor, neuropilin-1, is essential for the initiation of the primary immune response. Nat Immunol. 2002; 3:477–482. [PubMed: 11953749]
14. Bruder D, Probst-Kepper M, Westendorf AM, Geffers R, Beissert S, Loser K, et al. Neuropilin-1: a surface marker of regulatory T cells. Eur J Immunol. 2004; 34:623–630. [PubMed: 14991591]
15. Bagri A, Tessier-Lavigne M, Watts RJ. Neuropilins in tumor biology. Clinical cancer research : an official journal of the American Association for Cancer Research. 2009; 15:1860–1864. [PubMed: 19240167]
16. Staton CA, Kumar I, Reed MW, Brown NJ. Neuropilins in physiological and pathological angiogenesis. J Pathol. 2007; 212:237–248. [PubMed: 17503412]
17. Pan Q, Chanthery Y, Liang WC, Stawicki S, Mak J, Rathore N, et al. Blocking neuropilin-1 function has an additive effect with anti-VEGF to inhibit tumor growth. Cancer Cell. 2007; 11:53–67. [PubMed: 17222790]
18. Pellet-Many C, Frankel P, Jia H, Zachary I. Neuropilins: structure, function and role in disease. Biochem J. 2008; 411:211–226. [PubMed: 18363553]
19. Bielenberg DR, Pettaway CA, Takashima S, Klagsbrun M. Neuropilins in neoplasms: expression, regulation, and function. Exp Cell Res. 2006; 312:584–593. [PubMed: 16445911]
20. Latil A, Bieche I, Pesche S, Valeri A, Fournier G, Cussenot O, et al. VEGF overexpression in clinically localized prostate tumors and neuropilin-1 overexpression in metastatic forms. Int J Cancer. 2000; 89:167–171. [PubMed: 10754495]
21. Binetruy-Tournaire R, Demangel C, Malavaud B, Vassy R, Rouyre S, Kraemer M, et al. Identification of a peptide blocking vascular endothelial growth factor (VEGF)-mediated angiogenesis. The EMBO journal. 2000; 19:1525–1533. [PubMed: 10747021]
22. Starzec A, Vassy R, Martin A, Lecouvey M, Di Benedetto M, Crepin M, et al. Antiangiogenic and antitumor activities of peptide inhibiting the vascular endothelial growth factor binding to neuropilin-1. Life Sci. 2006; 79:2370–2381. [PubMed: 16959272]
23. Chang, BW.; Siccion, E.; Saif, MW. Updates in locally advanced pancreatic cancer. Highlights from the "2010 ASCO Annual Meeting"; Chicago, IL, USA. June 4–8, 2010; JOP 2010; 11; 313-316.
24. Lan MS, Batra SK, Qi WN, Metzgar RS, Hollingsworth MA. Cloning and sequencing of a human pancreatic tumor mucin cDNA. The Journal of biological chemistry. 1990; 265:15294–15299. [PubMed: 2394722]
25. Roy LD, Sahraei M, Subramani DB, Besmer D, Nath S, Tinder TL, et al. MUC1 enhances invasiveness of pancreatic cancer cells by inducing epithelial to mesenchymal transition. Oncogene. 2011; 30:1449–1459. [PubMed: 21102519]
26. Sahraei M, Roy LD, Curry JM, Teresa TL, Nath S, Besmer D, et al. MUC1 regulates PDGFA expression during pancreatic cancer progression. Oncogene. 2012; 31:4935–4945. [PubMed: 22266848]
27. Besmer DM, Curry JM, Roy LD, Tinder TL, Sahraei M, Schettini J, et al. Pancreatic ductal adenocarcinoma mice lacking mucin 1 have a profound defect in tumor growth and metastasis. Cancer Res. 2011; 71:4432–4442. [PubMed: 21558393]
28. Woo JK, Choi Y, Oh SH, Jeong JH, Choi DH, Seo HS, et al. Mucin 1 enhances the tumor angiogenic response by activation of the AKT signaling pathway. Oncogene. 2012; 31:2187–2198. [PubMed: 21927028]
29. Lau SK, Weiss LM, Chu PG. Differential expression of MUC1, MUC2, and MUC5AC in carcinomas of various sites: an immunohistochemical study. Am J Clin Pathol. 2004; 122:61–69. [PubMed: 15272531]
30. Parikh AA, Liu WB, Fan F, Stoeltzing O, Reinmuth N, Bruns CJ, et al. Expression and regulation of the novel vascular endothelial growth factor receptor neuropilin-1 by epidermal growth factor in human pancreatic carcinoma. Cancer. 2003; 98:720–729. [PubMed: 12910515]

31. Guidolin D, Vacca A, Nussdorfer GG, Ribatti D. A new image analysis method based on topological and fractal parameters to evaluate the angiostatic activity of docetaxel by using the Matrigel assay in vitro. Microvasc Res. 2004; 67:117–124. [PubMed: 15020202]
32. Moshal KS, Ferri-Lagneau KF, Leung T. Zebrafish model: worth considering in defining tumor angiogenesis. Trends Cardiovasc Med. 2010; 20:114–119. [PubMed: 21335280]
33. Hess-Stumpp H, Haberey M, Thierauch KH. PTK 787/ZK 222584, a tyrosine kinase inhibitor of all known VEGF receptors, represses tumor growth with high efficacy. Chembiochem : a European journal of chemical biology. 2005; 6:550–557. [PubMed: 15742376]
34. Solorzano CC, Baker CH, Bruns CJ, Killion JJ, Ellis LM, Wood J, et al. Inhibition of growth and metastasis of human pancreatic cancer growing in nude mice by PTK 787/ZK222584, an inhibitor of the vascular endothelial growth factor receptor tyrosine kinases. Cancer biotherapy & radiopharmaceuticals. 2001; 16:359–370. [PubMed: 11776753]
35. Takahashi T, Yamaguchi S, Chida K, Shibuya M. A single autophosphorylation site on KDR/Flk-1 is essential for VEGF-A-dependent activation of PLC-gamma and DNA synthesis in vascular endothelial cells. The EMBO journal. 2001; 20:2768–2778. [PubMed: 11387210]
36. Bernatchez PN, Soker S, Sirois MG. Vascular endothelial growth factor effect on endothelial cell proliferation, migration, and platelet-activating factor synthesis is Flk-1-dependent. The Journal of biological chemistry. 1999; 274:31047–31054. [PubMed: 10521504]
37. Shibuya M, Claesson-Welsh L. Signal transduction by VEGF receptors in regulation of angiogenesis and lymphangiogenesis. Exp Cell Res. 2006; 312:549–560. [PubMed: 16336962]
38. Nath S, Daneshvar K, Roy LD, Grover P, Kidiyoor A, Mosley L, et al. MUC1 induces drug resistance in pancreatic cancer cells via upregulation of multidrug resistance genes. Oncogenesis. 2013; 2:e51. [PubMed: 23774063]
39. Miao HQ, Lee P, Lin H, Soker S, Klagsbrun M. Neuropilin-1 expression by tumor cells promotes tumor angiogenesis and progression. FASEB J. 2000; 14:2532–2539. [PubMed: 11099472]
40. Mak P, Leav I, Pursell B, Bae D, Yang X, Taglienti CA, et al. ERbeta impedes prostate cancer EMT by destabilizing HIF-1alpha and inhibiting VEGF-mediated snail nuclear localization: implications for Gleason grading. Cancer Cell. 2010; 17:319–332. [PubMed: 20385358]
41. Prud'homme GJ. Cancer stem cells and novel targets for antitumor strategies. Curr Pharm Des. 2012; 18:2838–2849. [PubMed: 22390767]
42. Beck B, Driessens G, Goossens S, Youssef KK, Kuchnio A, Caauwe A, et al. A vascular niche and a VEGF-Nrp1 loop regulate the initiation and stemness of skin tumours. Nature. 2011; 478:399–403. [PubMed: 22012397]
43. Hamerlik P, Lathia JD, Rasmussen R, Wu Q, Bartkova J, Lee M, et al. Autocrine VEGF-VEGFR2-Neuropilin-1 signaling promotes glioma stem-like cell viability and tumor growth. J Exp Med. 2012; 209:507–520. [PubMed: 22393126]
44. Curry JM, Thompson KJ, Rao SG, Besmer DM, Murphy AM, Grdzelishvili VZ, et al. The use of a novel MUC1 antibody to identify cancer stem cells and circulating MUC1 in mice and patients with pancreatic cancer. J Surg Oncol. 2013; 107:713–722. [PubMed: 23335066]
45. Tinder TL, Subramani DB, Basu GD, Bradley JM, Schettini J, Million A, et al. MUC1 enhances tumor progression and contributes toward immunosuppression in a mouse model of spontaneous pancreatic adenocarcinoma. Journal of immunology. 2008; 181:3116–3125.
46. Xin Y, Li J, Wu J, Kinard R, Weekes CD, Patnaik A, et al. Pharmacokinetic and pharmacodynamic analysis of circulating biomarkers of anti-NRP1, a novel antiangiogenesis agent, in two phase I trials in patients with advanced solid tumors. Clinical cancer research : an official journal of the American Association for Cancer Research. 2012; 18:6040–6048. [PubMed: 22962439]
47. Weekes CD, Beeram M, Tolcher AW, Papadopoulos KP, Gore L, Hegde P, et al. A phase I study of the human monoclonal anti-NRP1 antibody MNRP1685A in patients with advanced solid tumors. Investigational new drugs. 2014; 32:653–660. [PubMed: 24604265]
48. Patnaik A, LoRusso PM, Messersmith WA, Papadopoulos KP, Gore L, Beeram M, et al. A Phase Ib study evaluating MNRP1685A, a fully human anti-NRP1 monoclonal antibody, in combination with bevacizumab and paclitaxel in patients with advanced solid tumors. Cancer chemotherapy and pharmacology. 2014; 73:951–960. [PubMed: 24633809]

49. Hingorani SR, Petricoin EF, Maitra A, Rajapakse V, King C, Jacobetz MA, et al. Preinvasive and invasive ductal pancreatic cancer and its early detection in the mouse. Cancer Cell. 2003; 4:437–450. [PubMed: 14706336]
50. Spicer AP, Rowse GJ, Lidner TK, Gendler SJ. Delayed mammary tumor progression in Muc-1 null mice. The Journal of biological chemistry. 1995; 270:30093–30101. [PubMed: 8530414]
51. Schroeder JA, Thompson MC, Gardner MM, Gendler SJ. Transgenic MUC1 interacts with epidermal growth factor receptor and correlates with mitogen-activated protein kinase activation in the mouse mammary gland. The Journal of biological chemistry. 2001; 276:13057–13064. [PubMed: 11278868]
52. Adham SA, Al Harrasi I, Al Haddabi I, Al Rashdi A, Al Sinawi S, Al Maniri A, et al. Immunohistological insight into the correlation between neuropilin-1 and epithelial-mesenchymal transition markers in epithelial ovarian cancer. The journal of histochemistry and cytochemistry : official journal of the Histochemistry Society. 2014; 62:619–631. [PubMed: 24850663]
53. Moshal KS, Ferri-Lagneau KF, Haider J, Pardhanani P, Leung T. Discriminating different cancer cells using a zebrafish in vivo assay. Cancers (Basel). 2011; 3:4102–4113. [PubMed: 24213127]

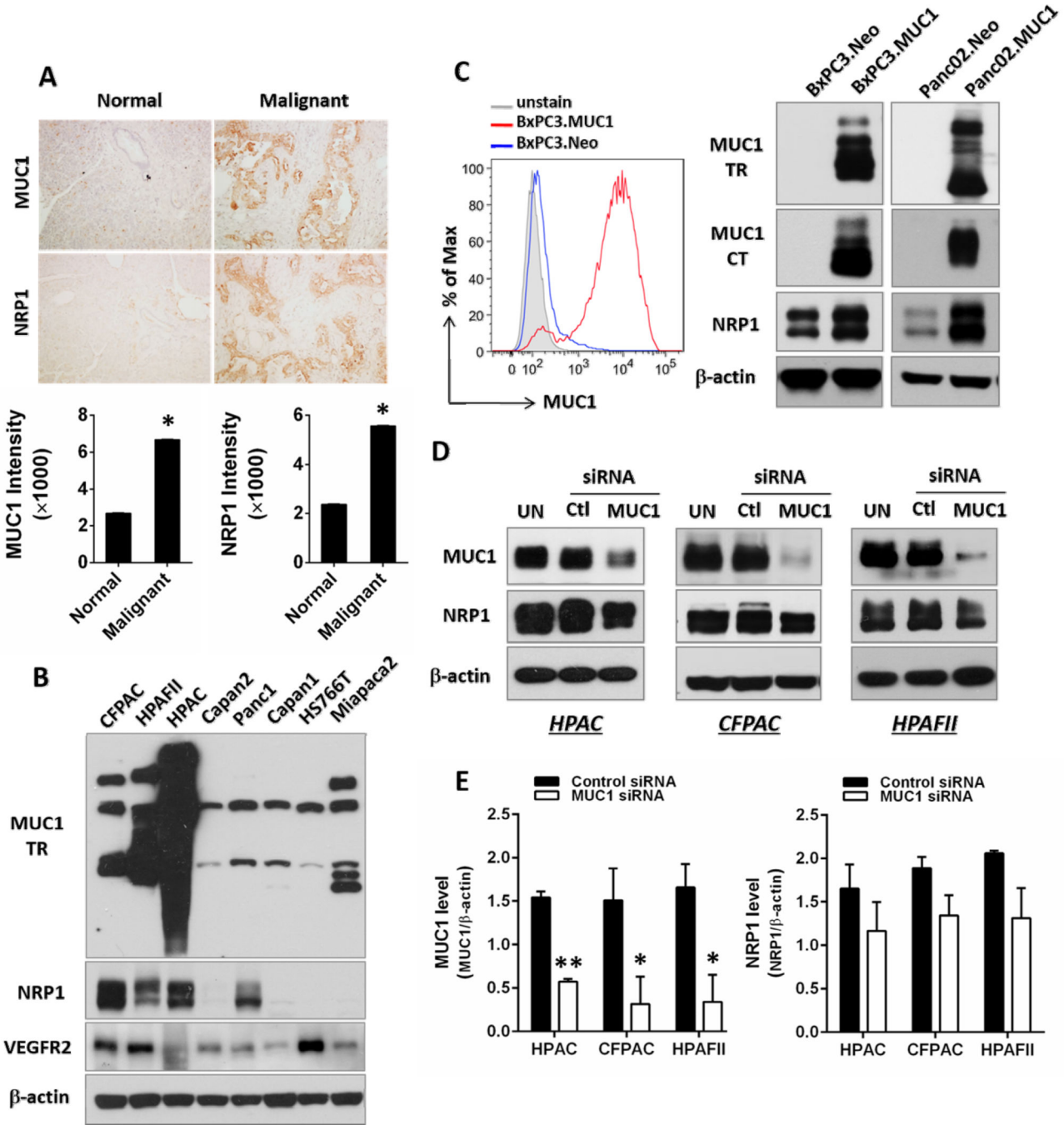

Figure 1. In PDA, tMUC1/Muc1 may regulate NRP1 protein expression

(A) Immunohistochemistry staining in human pancreas tissues. The top panels show representative images, and the bottom panels show the intensity quantitation for protein expression. **(B)** Western blot of total cell lysates from a panel of human pancreatic cell lines. β-actin was included as control for equal loading of protein. **(C)** Gain of function. BxPC3 (human) and Panc02 (murine) PDA cell lines were stably transfected with full length human MUC1. Left panel, tMUC1 expression in BxPC3 cells analyzed by flow cytometry. Cells were left unstained or stained with tMUC1-specific TAB004 antibody. Right panel, tMUC1

and NRP1 expression analyzed by Western blot. TR, tandem repeat; CT, cytoplasmic tail. **(D)** Loss of function. Western blot of cell lysates from tMUC1^{hi} cells treated with control siRNA (Ctl), MUC1-specific siRNA (MUC1), or left untreated (UN) for 48hr (in HPAFII) or 72hr (in HPAC and CFPAC). **(E)** The quantitation of repeated experiments for (D) with ImageJ software. *p<0.05; **p<0.01.

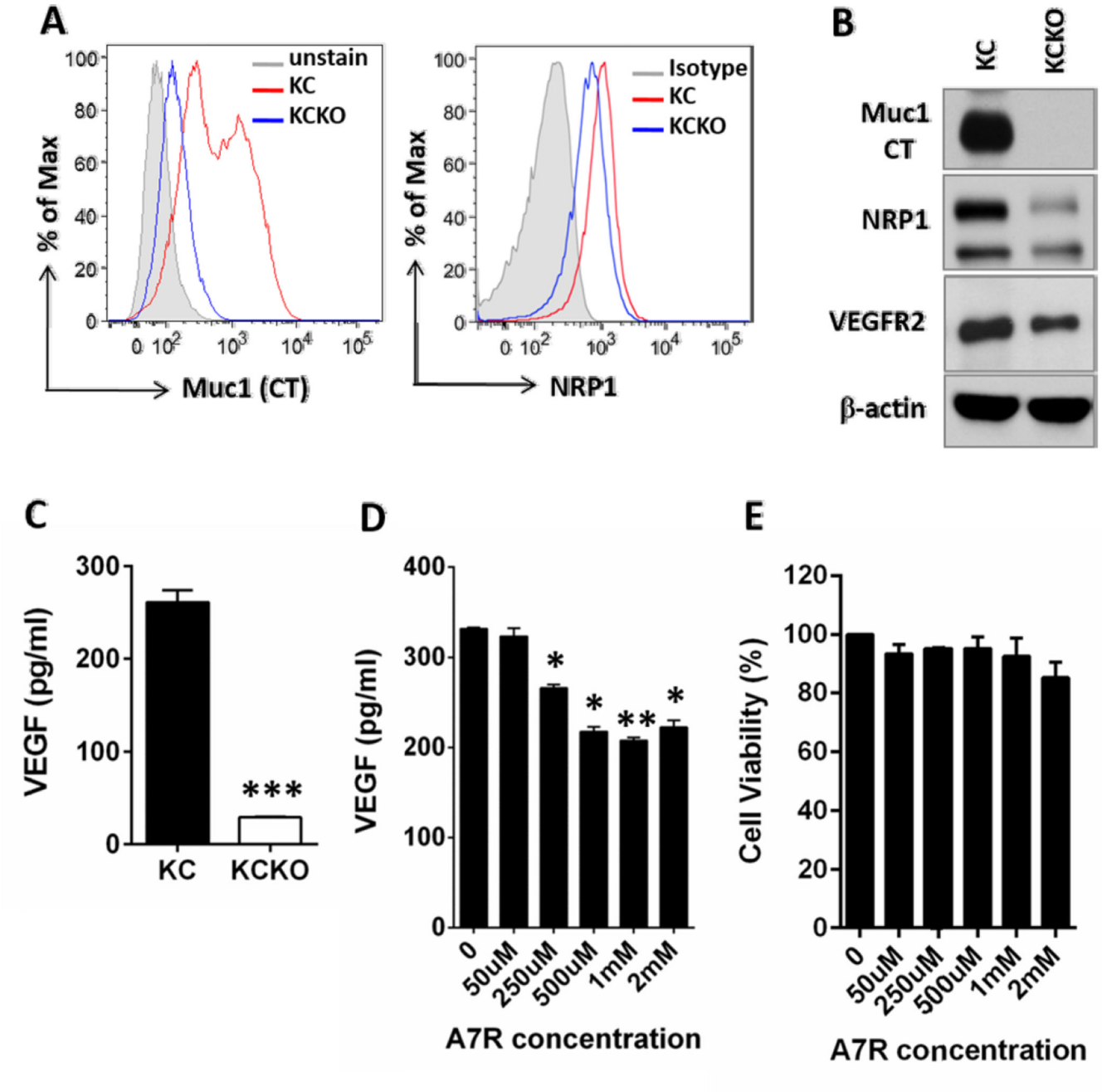

Figure 2. Muc1-expressing spontaneous mouse PDA cells have increased NRP1 expression and VEGF production

(A) KC cells were positive for Muc1 and expressed higher NRP1 than KCKO cells by flow cytometry analysis. **(B)** The expression of Muc1, NRP1, and VEGFR2 were assessed in cell lysates by Western Blot. **(C)** KC cells produced more VEGF determined by ELISA. ***p<0.001. **(D)** NRP1 antagonist A7R suppressed VEGF production in KC cells. *p<0.05; **p<0.01. **(E)** No significant effect of A7R on KC cell viability determined by MTT assay.

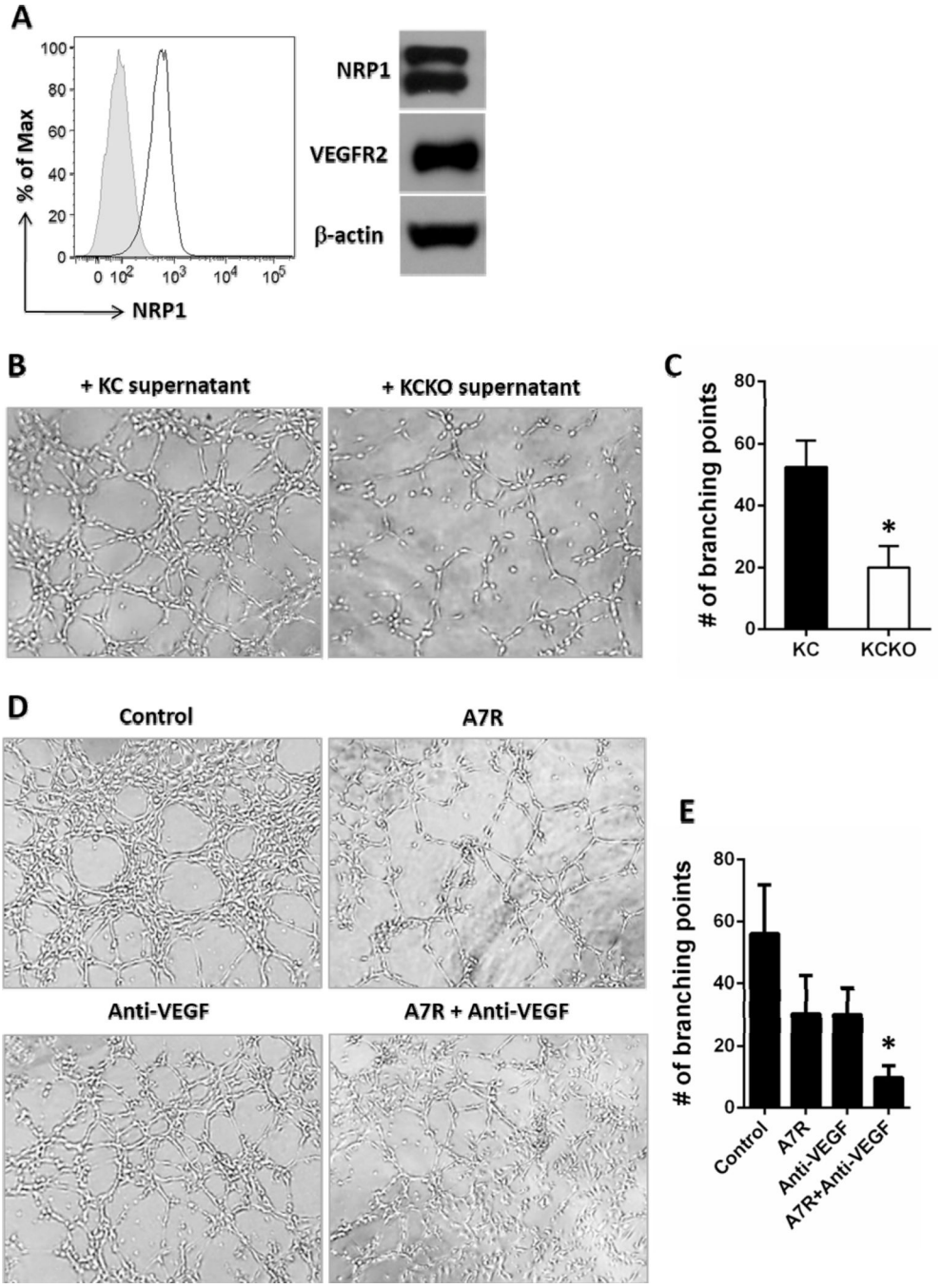

Figure 3. KC cell-conditioned medium induces stronger tube formations in 2H11 endothelial cells which can be reversed by blocking VEGF signaling

(A) 2H11 cells expressed NRP1 and VEGFR2, determined by flow cytometry (left panel) and Western blot (right panel). **(B)** KC ($Muc1^{hi}$) cell conditioned medium induced more capillary-like structure in 2H11 cells. **(C)** Quantitation of tube formation in **(B)** with ImageJ. *p<0.05. **(D)** Reversal of tube formation by NRP1 blockade and VEGF neutralization. KC cell-conditioned medium was pre-incubated with 500μM of A7R and/or 2μg/ml of anti-

VEGF antibody for 2hr before adding to 2H11 cells on Matrigel. **(E)** Quantitation of tube formation in **(D)**.

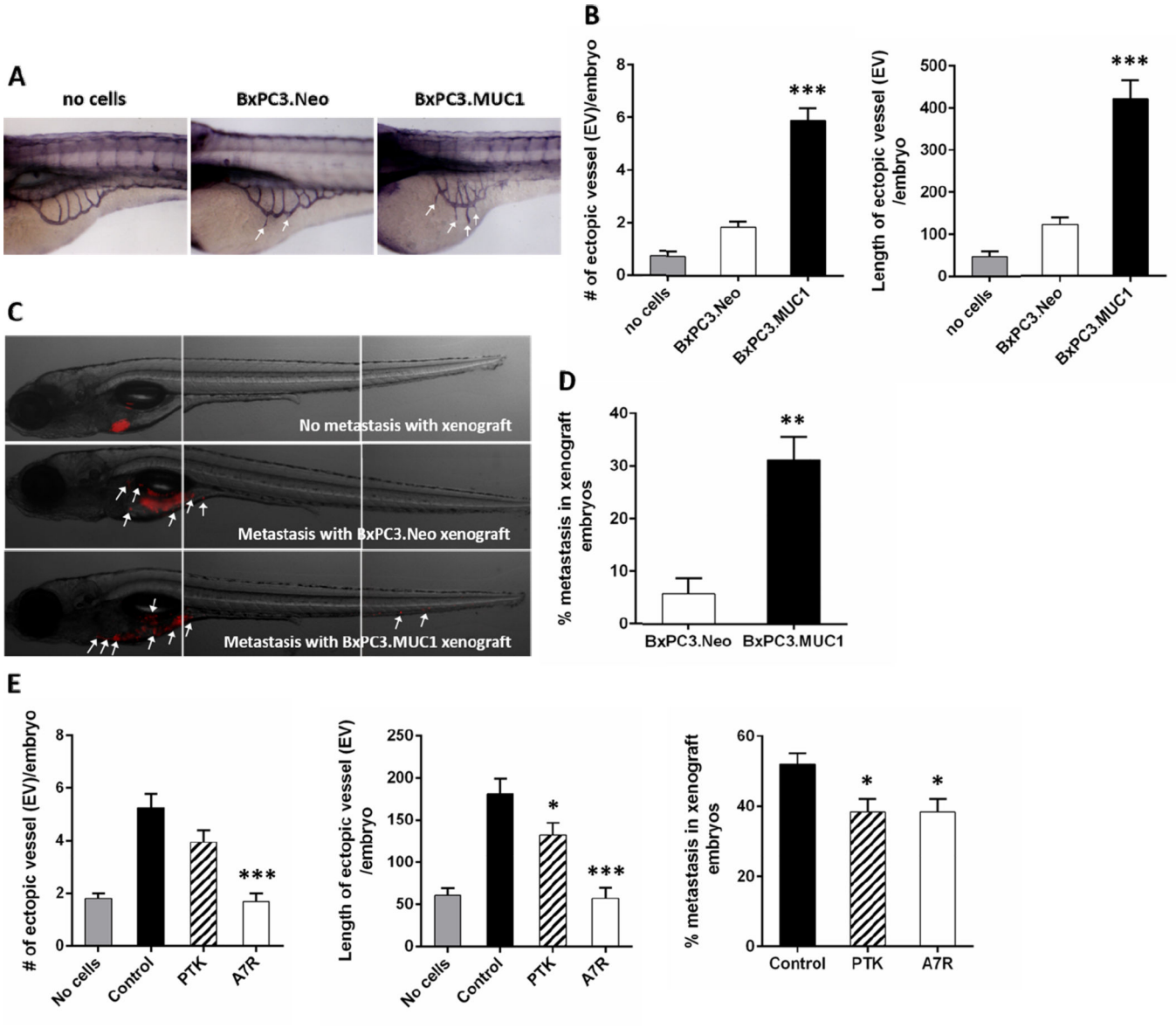

Figure 4. NRP1 is essential in promoting ectopic blood vessel formation and enhancing tumor cell metastasis in a zebrafish embryo xenograft model

(A) Representative images of zebrafish embryo with formation of new ectopic blood vessels, as pointed with white arrows. **(B)** Quantitative measurement of number and length of ectopic vessels formed in the embryo. ***p<0.001 between BxPC3.Neo group and BxPC3.MUC1 group. **(C)** Representative images of zebrafish embryo with metastatic lesions. The metastatic spread of tumor cells from the site of injection was pointed with white arrows. **(D)** The percentage of metastasis in the embryo. **p<0.01 between BxPC3.Neo group and BxPC3.MUC1 group. (E) Suppression of ectopic vessel formation (length and number) and metastatic spread in embryo by VEGFR or NRP1 antagonists. Statistics was performed between control and treatment groups.

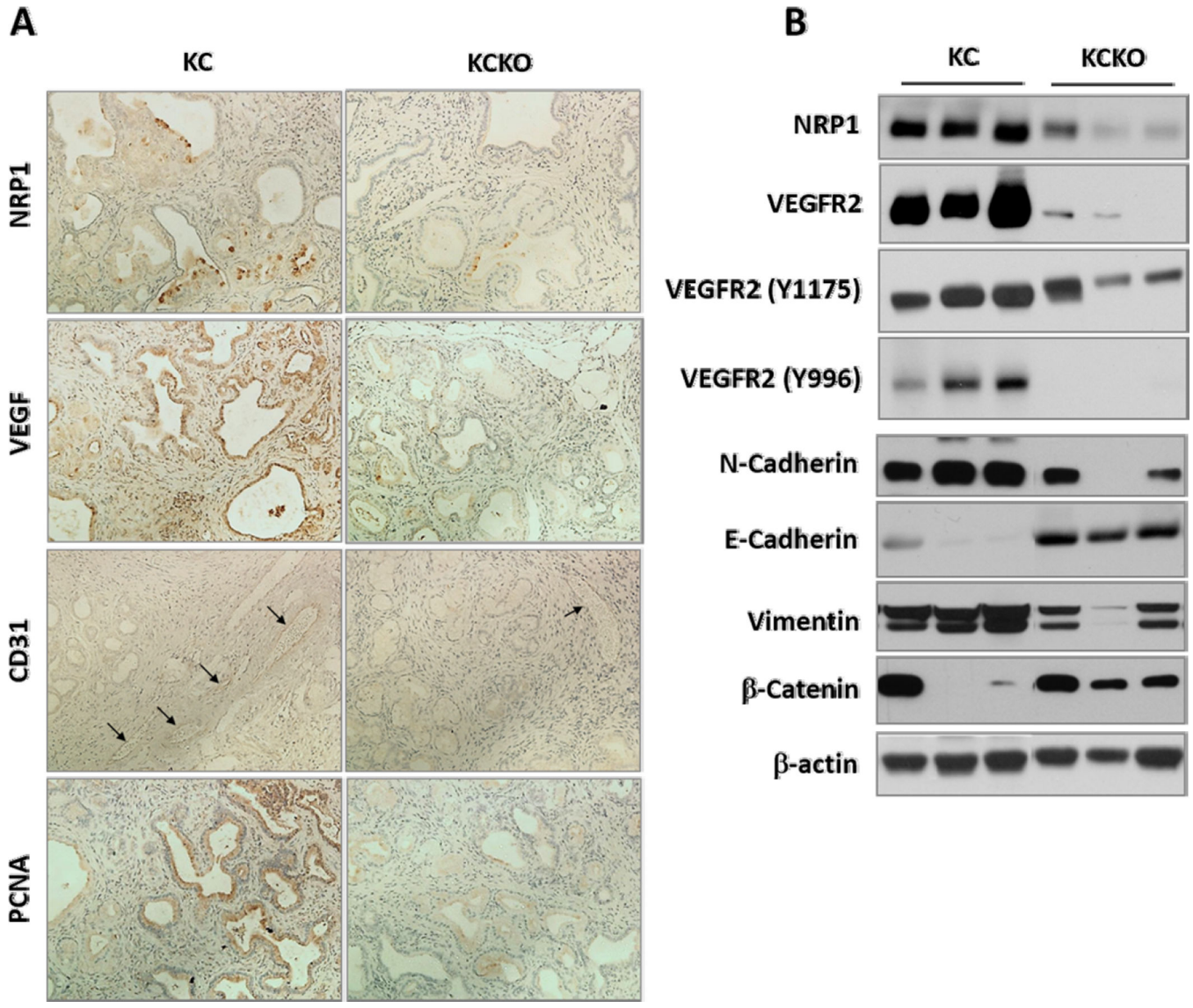

Figure 5. tMUC1 enhances proteins associated with angiogenesis and EMT

(A) Higher expression of angiogenesis-associated proteins in spontaneously developed KC tumor compared to KCKO tumor. **(B)** Higher VEGF signaling and EMT switch in Muc1-expressing KC tumor. KC and KCKO cells were subcutaneously injected into C57BL/6 mice. After twenty-six days, tumors were collected and lysates were analyzed by Western blot. Data from 3 mice out of 6–8 mice was shown.

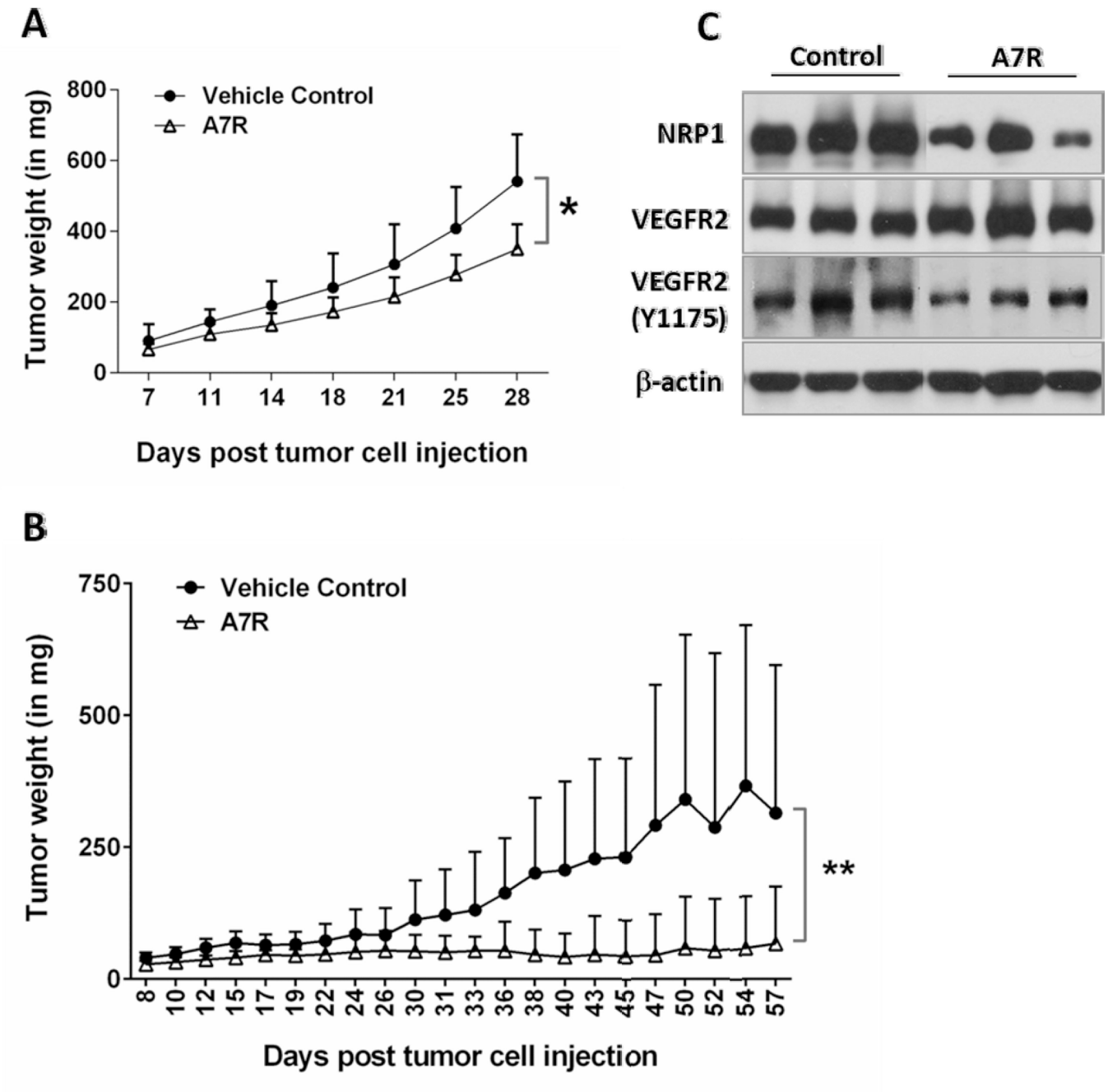

Figure 6. NRP1 antagonist A7R retards tumor growth *in vivo*

(A) Treatment with A7R attenuated KC tumor growth in C57BL/6 mice. *p<0.05. **(B)** A7R attenuated BxPC3.MUC1 tumor growth in nude mice. **p<0.01. **(C)** A7R treatment *in vivo* reduced NRP1 level as well as VEGFR2 phosphorylation at Tyr1175. Data from 3 mice out of 7 mice is shown.

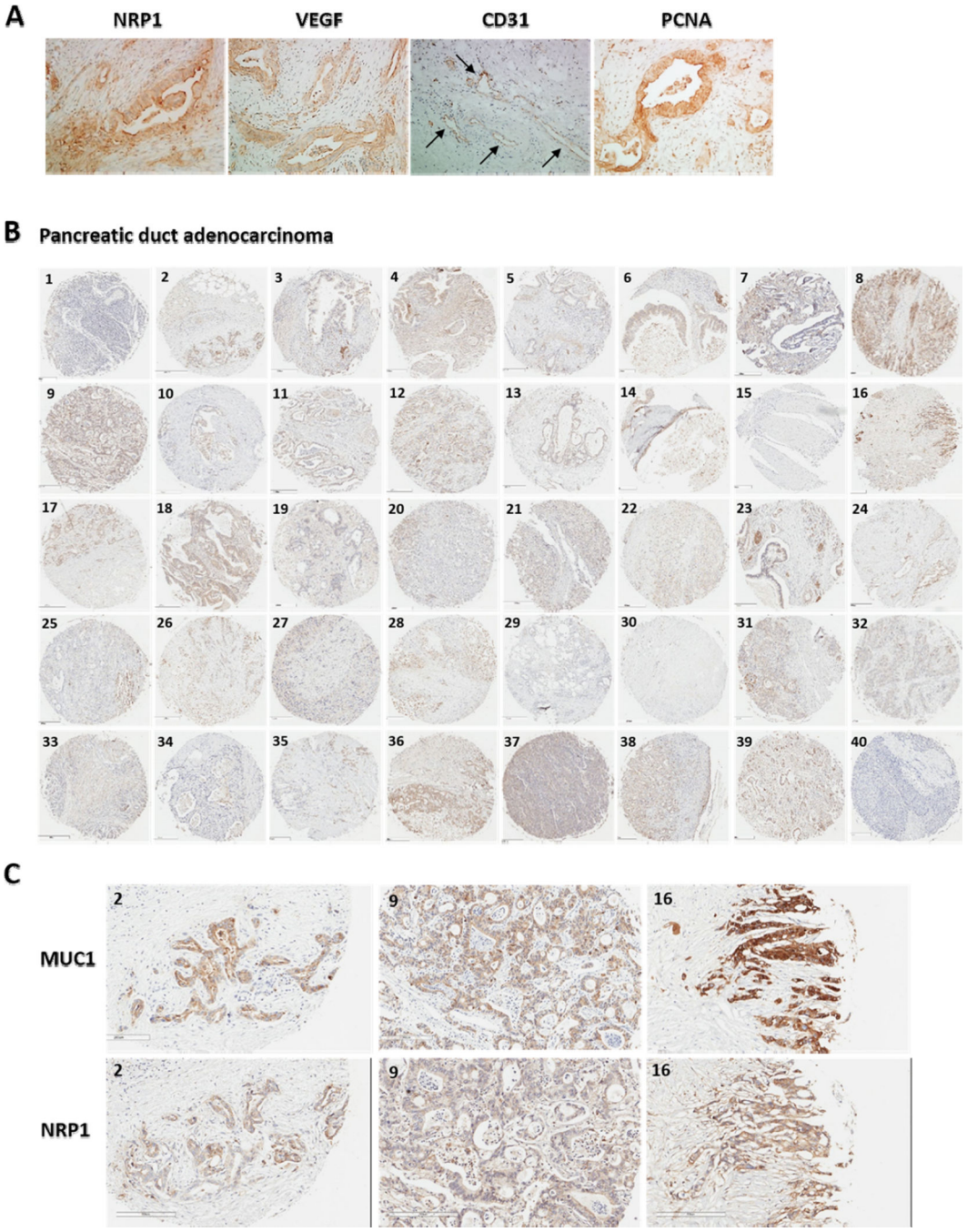

Figure 7. Primary human PDA tumors express NRP1 and other angiogenesis-associated proteins

(A) High expression of angiogenesis-associated proteins in primary human PDA tissue. The $CD31^{+}$ vessels were pointed by black arrows. **(B)** Pancreas tissue microarray for NRP1 expression. Representative images of n=40 PDA cores were shown at 40× magnification. The pathologic/diagnostic information was provided in supplementary Table1. **C)** MUC1 and NRP1 staining in PDA tissues from the same patients: Images from cores 2, 9, and 16 were shown at higher magnification. Using 65 such cores, a nonparametric Spearman

correlation of 0.70 was achieved which was highly significant ($P < 0.0001$) and indicates a positive association between the two biomarkers (Supplemental Figure 6).